Desalination and Water Treatment
www.deswater.com
doi: 10.1080/19443994.2015.1007486

57 (2016) 6310–6319
March

Taylor & Francis
Taylor & Francis Group

Optimization and modeling of preparation conditions of poly-Si-Fe-Zn (PSFZ) coagulant from industrial wastes using response surface methodology

Ming Li, Yanzhen Yu*, Yan Feng, Juan Tan

School of Civil Engineering and Architecture, University of Jinan, Jinan 250022, China, Tel./Fax: +86 53189736600; emails: liming8806@126.com (M. Li), yu_yan_zhen@126.com (Y. Yu), lm52lm@163.com (Y. Feng), tanjuan745@gmail.com (J. Tan)

Received 27 April 2014; Accepted 6 January 2015

ABSTRACT

A new composite coagulant poly-Si-Fe-Zn (PSFZ) was synthesized using industrial wastes as main raw materials and parameters affecting the coagulant performance, such as polymerization temperature, time, and Si/(Fe + Zn) moral ratio in this study, were examined. In addition, to obtain the optimum preparation conditions resulting in the maximum turbidity and ammonia nitrogen (NH_3-N) removal, response surface methodology was used to assess their interactive effects on coagulation performance, and quadratic models based on the high value (>0.97) of determination coefficient (R^2) were conducted for the response variables: turbidity and NH_3-N removal efficiency. The results showed that optimum preparation conditions were found to be polymerization temperature of 65°C, polymerization time of 80 min, and Si/(Fe + Zn) moral ratio of 0.73, corresponding to predicted turbidity and NH_3-N removal percentages of 96 and 77.03, respectively. Besides, the structure and morphology of PSFZ were characterized by X-ray diffraction, infrared spectroscopy, and scanning electron microscope. The comparison between quadratic regression equations of turbidity and NH_3-N removal was evaluated using interpolation method, in which the optimized preparation conditions were proved to be suitable with deviation error of 2–4%.

Keywords: Poly-Si-Fe-Zn coagulant; Industrial wastes; Response surface methodology; Turbidity and NH_3-N removal

1. Introduction

In recent years, eutrophication caused by increasing nitrogen and phosphorus has become a severe environmental problem that human beings face. Therefore, investigation on nitrogen and phosphorus removal has attracted more and more attention in the field of wastewater treatment [1]. There are two ways to remove ammonium nitrogen in general: physicochemical and biological methods, where biological method is used widely [2]. But there still existed some problems in conventional biological denitrification process: high consumption of oxygen and energy, unstable operation, etc. [3,4]. Compared with biological method, chemical method has the advantages of high efficiency and wide application rage [5]. Accordingly, to overcome these difficulties, a physicochemical technology was studied in this work to remove nitrogen, in which a new coagulant prepared from industrial wastes was probed.

*Corresponding author.

Solid industrial waste pollution is increasingly serious. Coal fly ash is generated as an industrial waste in the process of coal combustion in thermal power plant, and their production was estimated to be 780 Mt annum [6]. Fly ash consists of silicon, iron, aluminum, calcium, and a few other compounds, such as magnesium, sodium, and potassium oxides. The sum of silicon, aluminum, and iron oxides can commonly be as high as 80% [7,8]. In addition, Galvanized iron slag generated from galvanized industry is a solid waste, which consist of zinc, iron, and other metals. As far as we know, iron and zinc are important metal elements to prepare inorganic coagulant [9]. Therefore, the preparation of poly-Si-Fe-Zn (PSFZ) using industrial wastes has its practical basis.

Conventionally, the optimization of multifactor experiments is generally carried out by varying a single factor while keeping the other factors fixed at a specific set of condition. This experimental design is time-consuming and incapable of effective optimization. In recent years, response surface methodology (RSM) has been employed to develop, improve, and optimize the experimental design based on a collection of statistical and mathematical technique. The main advantage of RSM is the reduced number of experimental trials required to assess multiple parameters and their interactions [10,11]. The application of this method on the development of suitable water treatment is rarely reported.

In this work, the composite coagulant PSFZ coagulant was synthesized using industrial wastes. In order to optimize the preparing conditions, the effect of polymerization temperature, time, and Si/(Fe + Zn) moral ratio on turbidity and NH_3-N removal efficiency was investigated, while the RSM was employed to study their mutual effect and obtain the optimum preparation conditions. In addition, the characterization of PSFZ was analyzed by X-ray diffraction (XRD), infrared spectra (IR), and scanning electron microscope.

2. Materials and methods

2.1. Materials

The industrial wastes used in this study include coal fly ash and galvanized iron slag, which were obtained from Huang Tai Thermal Power Plant and Zhongguan Galvanized Iron Plant (China), respectively. The compositions of the wastes are shown in Table 1. Coal fly ash and galvanized iron slag compositions are determined by WFX–130A Atomic absorption spectrophotometer (Beifen-Ruili, China).

2.2. Preparation of PSFZ coagulant

Preparation of PSFZ could be divided into the following steps.

2.2.1. Pretreatment

Firstly, 85 mL NaOH solution (50% (*w*/*w*), analytical grade) was introduced into 20 g fly ash which was screened with 200 mesh sieve, and was followed by leaching of 60 min in SHA-B Thermostatic Water Bath (Jintan Ronghua Instrument) at 90˚C to obtain leaching solution. The Si_2O concentration was determined by potassium fluorosilicate method (GB/T 176-2008, China) to be 0.53 mol/L.

Eighty-seven milliliter H_2SO_4 solution (35% (*w*/*w*), analytical grade) and 16 g galvanized iron slag which was smashed into irregular regiment massive with equivalent diameter from about 0.5 to 1.5 cm were added into a beaker, heated under stirring to 80˚C, and kept for 90 min. After that, the mixture was filtered. The Fe^{3+} and Zn^{2+} concentration were obtained by EDTA titration (GB/T 176-2008, China) to be 0.43 and 0.22 mol/L, respectively.

2.2.2. Polymerization

Various amounts of water glass solution were introduced slowly into the metal salt solution. Then NaOH solution (0.5% (*w*/*w*), analytical grade) was added to the mixture to polymerize 60–120 min under 50–80˚C and stirred to obtain a liquid product of PSFZ with pH 1.5. The solution was aged for 48 h at normal temperature and PSFZ was obtained.

2.3. Characteristics of coagulants

The samples of liquid coagulants were dried at 60˚C for 48 h and ground into powders, which were analyzed by KBr pressed disk with Nicolet Tensor 27 IR Spectrum Meter (Bruker, German) and measured with a D/MAXRB XRD Meter (Rigaku, Japan). The surface morphology of solid PSFZ was observed and analyzed by S-2500 SEM (Hitachi, Japan) at 5,000× magnification.

2.4. Flocculation test

The water sample was collected from a landscape lake located in campus of University of Jinan. 23.31 mg/L ammonium chloride was added into the raw water sample due to the low concentration of nitrogen and was followed by 10 min stirring mixing.

Table 1
Composition of industrial wastes (wt.%)

Composition	SiO_2	Fe_2O_3	Al_2O_3	CaO	MgO	ZnO	SO_3	K_2O	Other
Coal fly ash	49.9	13.1	26.2	2.56	0.95	0.83	0.78	1.44	4.18
Galvanized iron slag	0.65	58.47	1.54	–	–	38.92	–	–	0.42

Supernatant was taken after settling 60 min as the tested water sample. Then the tested water sample with turbidity of 101 NTU, UV_{254} of 0.023 cm^{-1}, NH_3-N of 7.45 mg/L, CODcr of 148 mg/L, and pH of 7.89 was obtained.

Coagulation-flocculation experiment with a six-unit multiple stirrer system (JJ-4A, China) was performed at the room temperature and the dose of PSFZ was 95 mg/L (as Fe + Zn). The dose of coagulant was determined by pre-experiment. Coagulant was added to the tested sample (1 L), and the standard flocculation test procedure consisted of a rapid mix at 250 r/min for 1 min after chemical addition, followed by two 10 min mixing periods at 40 and 20 r/min, respectively. Then, the floc was allowed to settle for 10 min and 200 mL supernatant sample was withdrawn from a position of 3 cm below the surface. Finally, turbidity and NH_3-N were measured with SZD-2 Turbidity Meter (Shanghai, China) and Nessler's reagent colorimetric method using 752S Spectrophotometer (Beijing, China), respectively.

2.5. Experimental design

The preparation conditions for PSFZ coagulant was developed, modeled and optimized following the RSM which was used to find the relationship between one or more response variables and a set of quantitative, experimental variables or factors. Box-Behnken is a suitable design for sequential experiments to evaluate appropriate information for testing lack of fit without a large number of design points [12,13]. In this study, the Box-Behnken with three factors (temperature, time, and Si/(Fe + Zn)) was utilized to determine the effect of dependent factors, which include responses of turbidity and NH_3-N removal efficiency.

The three factors, or independent variables, were coded at three levels between −1 and +1, where −1 and +1 correspond to the minimum and maximum value of each variable, respectively, as noted in Table 2. For statistical calculations, the variable X_i was coded as Z_i according to the following equation:

$$Z_i = \frac{X_i - X_0}{\Delta X_i} \quad (1)$$

Table 2
The experimental domain factor and level for the Box-Behnken design

		Range and levels (coded)		
Factors		−1	0	+1
Temperature (°)	X_1	50	65	80
Time (min)	X_2	60	90	120
Si/(Fe + Zn)	X_3	0.6	0.8	1.0

X_i is independent variable real value, X_0 is independent variable real value in center point of the independent variable and ΔX_i is the step change in X_i. Thus, the coded variables range from −1 to +1.

According to Box-Behnken experimental design, the investigation was carried out through 17 experimental runs as presented in Table 3 using the Design-Expert 8.0.6 (Stat-Ease Inc., Minneapolis, USA).

To formulate a simple model suitable for optimization, the response is related to the selected variables by linear and quadratic terms, as follows:

$$Y = \beta_0 + \sum_{i=1}^{k} \beta_i X_i + \sum_{i=1}^{k} \beta_{ii} X_i^2 + \sum_{1 \le i \le j \le k} \beta_{ij} X_i X_j + e_i \quad (2)$$

Y is the response, X_i and X_j are the factors, β_0 is a constant coefficient, β_i, β_{ii} and β_{ij} are the interaction coefficients of linear, quadratic, and second-order terms, respectively, k is the number of studied factors, and e_i is the error. ANOVA was executed to obtain the process factors and the response. The R^2 and adjusted R^2 (R^2_{adj}) were calculated to find out the goodness of fit of the model, and statistical significance was evaluated by the F-value and P-value [14].

3. Results and discussion

3.1. Regression model and statistical analysis

The experimental results were evaluated with Design-Expert 8.0.6 and the program recommended the use of a quadratic model form for all dependent

Table 3
The Box-Behnken design matrix for experimental design, observed, and predicted responds

Run no.	Real (coded) values			Response (Y %)			
				Turbidity removal		NH_3-N removal	
	X_1 (℃)	X_2 (min)	X_3	Predicted	Experiment	Predicted	Experiment
1	50(−1)	60(−1)	0.8(0)	93.98	94.21	70.34	71.13
2	80(1)	60(−1)	0.8(0)	94.77	94.83	65.22	65.30
3	50(−1)	120(1)	0.8(0)	90.55	90.49	66.16	66.08
4	80(1)	120(1)	0.8(0)	93.82	93.59	65.90	65.11
5	50(−1)	90(0)	0.6(−1)	91.08	90.82	71.52	70.48
6	80(1)	90(0)	0.6(−1)	93.86	93.77	66.68	66.36
7	50(−1)	90(0)	1.0(1)	93.71	93.80	59.79	60.11
8	80(1)	90(0)	1.0(1)	94.98	95.24	59.25	60.28
9	65(0)	60(−1)	0.6(−1)	93.56	93.59	75.98	76.23
10	65(0)	120(1)	0.6(−1)	92.16	92.48	66.47	67.58
11	65(0)	60(−1)	1.0(1)	96.21	95.89	58.64	57.53
12	65(0)	120(1)	1.0(1)	93.25	93.22	64.65	64.40
13	65(0)	90(0)	0.8(0)	96.38	96.58	75.66	75.86
14	65(0)	90(0)	0.8(0)	96.38	95.51	75.66	74.38
15	65(0)	90(0)	0.8(0)	96.38	96.80	75.66	76.50
16	65(0)	90(0)	0.8(0)	96.38	96.49	75.66	75.88
17	65(0)	90(0)	0.8(0)	96.38	96.52	75.66	75.68

variables. In terms of actual factors, empirical relationships between turbidity, and NH_3-N removal and the independent variables can be expressed as shown in Eqs. (3) and (4):

$$Y_1 = 23.746 + 1.052X_1 + 0.197X_2 + 67.860X_3 + 0.002X_1X_2 - 0.126X_1X_3 - 0.065X_2X_3 - 0.008X_1^2 - 0.002X_2^2 - 30.719X_3^2 \quad (3)$$

$$Y_2 = -42.353 + 2.525X_1 - 0.059X_2 + 131.056X_3 + 0.003X_1X_2 + 0.358X_1X_3 + 0.647X_2X_3 - 0.024X_1^2 - 0.004X_2^2 - 147.781X_3^2 \quad (4)$$

Table 4 displays the ANOVA results for the regression model and respective model items. As indicated in Table 4, the quadratic models obtained were significant, as indicated by the low probability values (P-value < 0.0001). Values of P-value less than 0.0500 indicate model terms are significant, while values greater than 0.10 indicate that the model terms are not significant. In this case, from Table 4 it is clear that the linear terms for X_1, X_2, and X_3 have large effects on turbidity removal as X_1 and X_3 on NH_3-N removal. The quadratic terms for X_1^2, X_2^2, and X_3^2 are also significant on all of the dependent variables. In addition, the interaction terms for X_1X_2 and X_2X_3 are significant on turbidity and NH_3-N removal, respectively. Furthermore, the lack of fit F-values of 0.64 and 3.4 obtained was statistically significant for turbidity and NH_3-N removal, respectively, because their p-values were less than 0.05. A high R^2 value, close to 1, ensures a satisfactory adjustment of the quadratic model to the experimental data. The values of the determination coefficient R^2 were 0.9748 and 0.9864 for turbidity and NH_3-N removal, respectively, all of which are greater than 0.80. The determination coefficient R^2 should be at least 0.80 for a good model fit.

Fig. 1 shows normal probability plots of the studentized residuals for turbidity and NH_3-N removal, respectively. The straight line formed in Fig. 1 indicates that the studentized residuals follow a normal distribution. If the residuals do not follow a distribution, an S-shape curve is formed, and this type of curve often results from the use of an incorrect model [15].

Fig. 2 plot the studentized residuals vs. predicted responses. This plot is expected to be a random scatter, indicating that the variation in the original observations is not related to the value of response. And the random scattering of the residuals in Fig. 2 shows that the suggested model is an appropriate description of the process.

Table 4
ANOVA for the regression model and respective model terms

Source	DF	Turbidity removal				NH_3-N removal			
		Sum of squares	Mean square	*F*-value	*p*-value	Sum of squares	Mean square	*F*-value	*p*-value
Model	9	57.47	6.39	30.13	<0.0001*	627.71	69.75	56.57	<0.0001*
X_1	1	8.22	8.22	38.79	0.0004*	14.45	14.45	11.72	0.0111*
X_2	1	9.55	9.55	45.05	0.0003*	6.16	6.16	5	0.0605*
X_3	1	7.01	7.01	33.09	0.0007*	183.65	183.65	148.96	<0.0001*
X_1X_2	1	1.54	1.54	7.25	0.0309*	5.9	5.9	4.79	0.0648*
X_1X_3	1	0.57	0.57	2.69	0.145**	4.6	4.6	3.73	0.0947**
X_2X_3	1	0.61	0.61	2.87	0.134**	60.22	60.22	48.84	0.0002*
X_1^2	1	12.8	12.8	60.4	0.0001*	124.66	124.66	101.11	<0.0001*
X_2^2	1	7.74	7.74	36.54	0.0005*	46.24	46.24	37.5	0.0005*
X_3^2	1	6.36	6.36	29.99	0.0009*	147.13	147.13	119.34	<0.0001*
Residual	7	1.48	0.21			8.63	1.23		
Lack of fit	3	0.48	0.16	0.64	0.6305	6.2	2.07	3.4	0.1342
Pure error	4	1.01	0.25			2.43	0.61		
Total	16	58.95				636.34			

$R^2_{\text{turbidityremoval}} = 0.9748$, $R^2_{\text{NH}_3\text{-N}} = 0.9864$.
*Significant at $p < 0.05$; **Significant at $p < 0.05$.

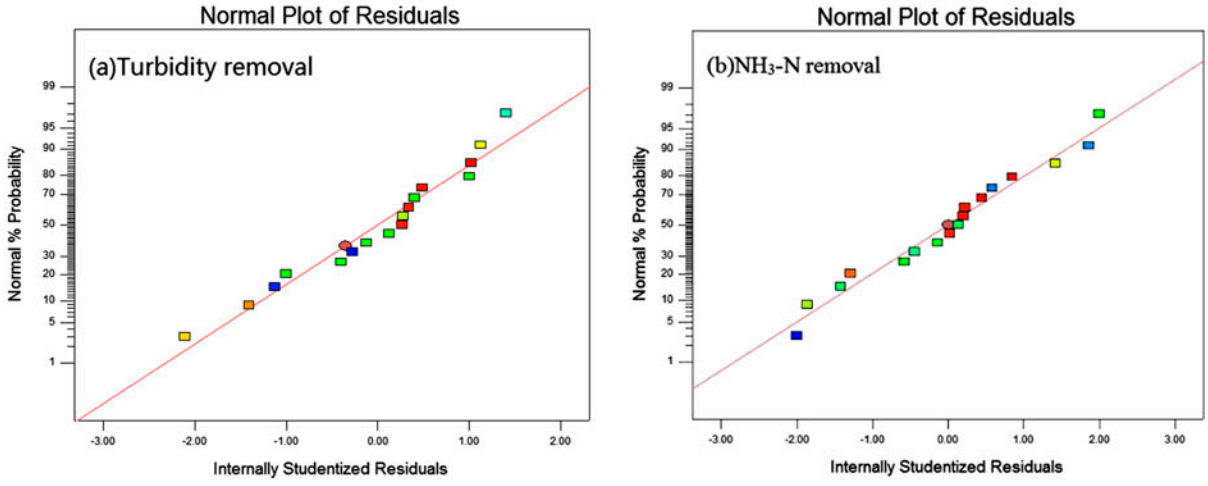

Fig. 1. Normal % probability and studentized residuals plot.

3.2. RSM analysis

In RSM analysis, the sensitivity of responses to the independent variables can be included by the there-dimensional (3D) graphs. Variables with the largest absolute coefficients in the models were chosen for the axes of the response surface plots. This was useful to visualize the relationship between the value of response and the level of each factor [16]. The influence of the three different process variables on turbidity and NH_3-N removal is shown in the 3D response surface plots.

3.2.1. RSM analysis on turbidity removal

Fig. 3 presents the relationship between turbidity removal and the independent variables X_1, X_2, and X_3.

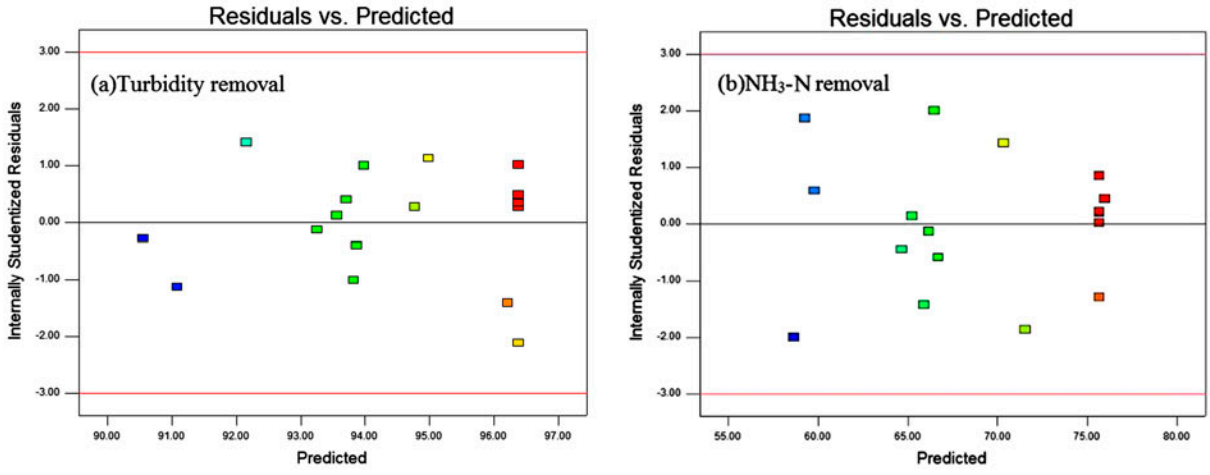

Fig. 2. The studentized residuals and predicted response plot.

Three-dimensional surface plots were formed based on the model polynomial function.

As indicated in Fig. 3(a), the removal of turbidity increased firstly with increasing of temperature from 50 to 65℃ and then was followed by a slow decrease from 65 to 80℃, in which other factors were involved in multiple interactions. The optimum temperature was 65℃ for turbidity removal with time of 90 min and Si/(Fe + Zn) of 0.8, in which the maximal removing rate of turbidity by PSFZ achieved about 96%. In addition, Fig. 3(a) shows the combined effects of temperature and time on turbidity removal based on the fitted second-order polynomial equation. The removal efficiency increased with increase of temperature ranging from 60 to 75℃ as well as with time ranging from 60 to 100 min and was found to be a function of the linear and quadratic effects of temperature and time. The linear effect ($p < 0.001$) and quadratic effect ($p < 0.001$) was positive, which resulted in a curvilinear increase on turbidity removal. Furthermore, the interaction effect ($p < 0.05$) between temperature and time was significant (Table 4).

As seen from Fig. 3(b) and (c), PAFZ give high removing turbidity effect, indicating that time and ratio of Si to (Fe + Zn) also have significant effect on turbidity removal, as noted in Table 4. PSFZ performed similar changing trend of turbidity removal to that of temperature: increased firstly and then was followed by a decrease. The mutual effect was performed in Fig. 3(b) and (c), indicating that increasing Si/(Fe + Zn) molar ratio, while decreasing the time could improve turbidity removal efficiency, especially at higher Si/(Fe + Zn) molar ratio and lower time. There was an increase in turbidity removal as ratio of Si to (Fe + Zn) increased within the investigated range of temperature.

3.2.2. RSM analysis on NH_3-N analysis

The relationship between NH_3-N removal and the operational variables X_1, X_2, and X_3 can be employed by 3D surface plots and Fig. 4 displays the 3D surface plots among the three factors.

Fig. 4(a) and (b) show the highest removal of NH_3-N by PSFZ coagulant was almost same with the temperature ranging from 55 to 72℃, time ranging from 65 to 105 min, and Si/(Fe + Zn) molar ratio ranging from 0.6 to 0.8. The mutual effects of independent variables also were obtained by Fig. 4(a) and (b). The decreasing of time and Si/(Fe + Zn) molar ratio could improve NH_3-N removal efficiency to some extent under certain temperature. However, according to ANOVA, the interaction between temperature and time ($p > 0.05$) as well as the interaction between temperature and Si/(Fe + Zn) moral ratio ($p > 0.05$) were insignificant.

Fig. 4(c) gives the performance of NH_3-N removal at varying time and moral ratio of Si to (Fe + Zn). It indicated that decreasing the Si/(Fe + Zn) moral ratio from 0.8 to 0.6 and time from 100 to 60 min could increase removal efficiency, especially at lower Si/(Fe + Zn) moral ratio and time. In addition, the linear effect of time ($p > 0.05$) was negative, whereas the quadratic effect ($p < 0.001$) was positive, which resulted in a curvilinear increase in NH_3-N removal. The Si/(Fe + Zn) moral ratio had a pronounced effect on response. The linear and quadratic effects were both positive, which explained the observed nature of

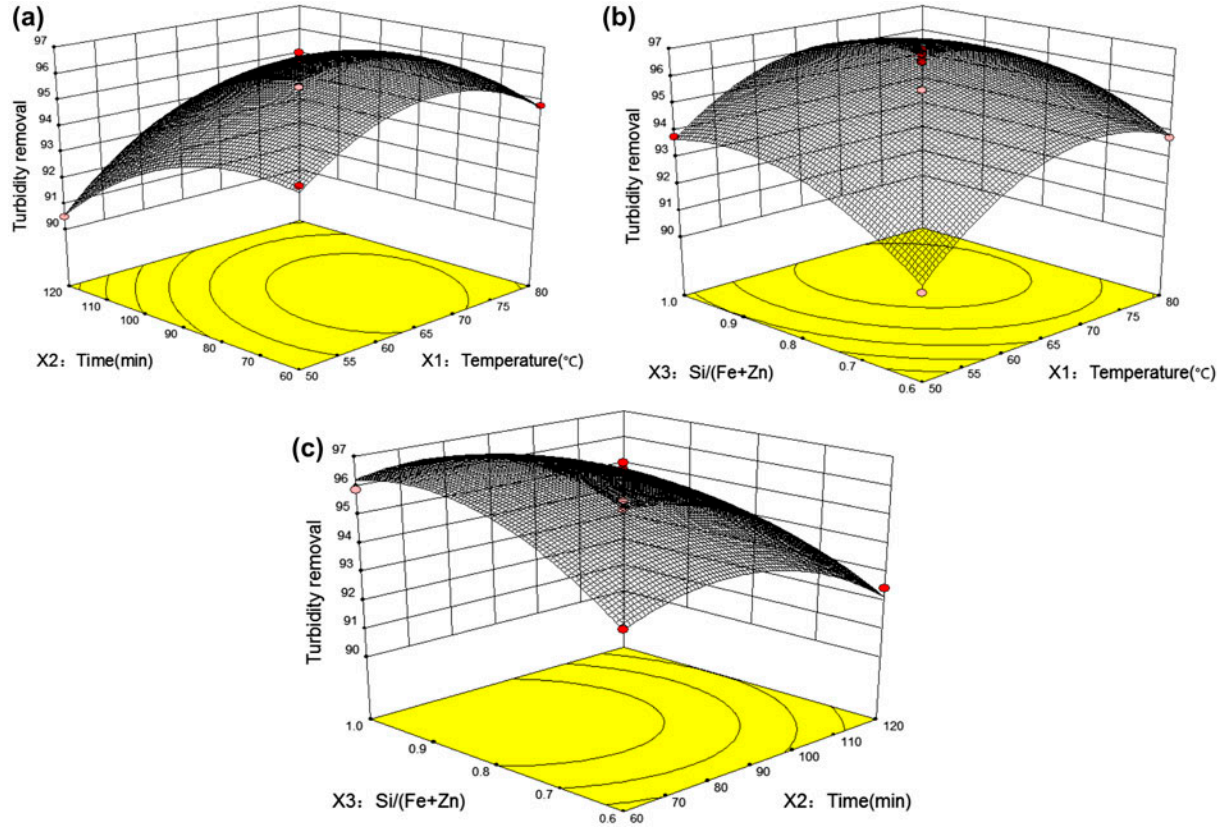

Fig. 3. Response surface for turbidity removal as a function of (a) temperature and time (Si/(Fe + Zn): 0.8), (b) temperature and Si/(Fe + Zn) (time: 90 min), and (c) time and Si/(Fe + Zn) (temperature: 65°C).

the curve. Besides, the interaction effect between time and moral ratio of Si to (Fe + Zn) ($p < 0.001$) was found to be extremely significant.

3.3. Characteristics of PSFZ

3.3.1. Analysis of IR spectra

Fig. 5 presents the IR spectra of PSFZ. The peak at 3,200–3,500 cm^{-1} is assigned to the intermolecular association stretching vibration of –OH [17]. The peaks at 1,632–1,640 cm^{-1} and 1,405–1,406 cm^{-1} could be attributed to the bending vibration of water absorbed, polymerized, and crystallized, while the former peak corresponds to the same peak at 1,631 cm^{-1} and the latter one corresponds to the same peak at 1,403 cm^{-1}. The above peaks increase in intensity. It implies that PSFZ contains massive –OH and –OH is mainly associated or free.

The peak at 1,138 cm^{-1} correspond to the asymmetric stretching vibration of Fe–OH–Fe or Zn–OH–Zn. PSFZ shows large absorption peaks at the above peak, probably because the peak position of Fe–OH–Fe or Zn–OH–Zn is affected by the folder angle and the adjacent elements. The wave at 988 cm^{-1} is attributed to the symmetrical stretching vibrations of Si–O–Fe and Si–O–Zn [18]. These bonds hydrolyze during coagulation and produce a hydroxyl complex with mono-core or multi-core silicon, and high abilities of neutralization, adsorption, and capture. Wavenumbers around 796 cm^{-1} correspond to the connection of tetrahedron of Si–O–Si, and are not present in the spectra of PSFZ, which suggest that PSFZ have a reticular formation. In addition, the peaks at 470–650 cm^{-1} are assigned to the bending vibrations of Fe–OH and Zn–OH and the winding vibration of Fe–O and Zn–O. These peaks disappear and are superimposed at 598 and 488 cm^{-1}, which suggest that Fe(III) and Zn(II) hydroxyl polymers are cross-copolymerized. Overall, the IR analysis results support the statement that PSFZ is a complex compound of Si and metal ions.

3.3.2. XRD analysis

Fig. 6 illustrates the XRD spectra of PSFZ. As shown in Fig. 6, various peaks can be observed, indicating a

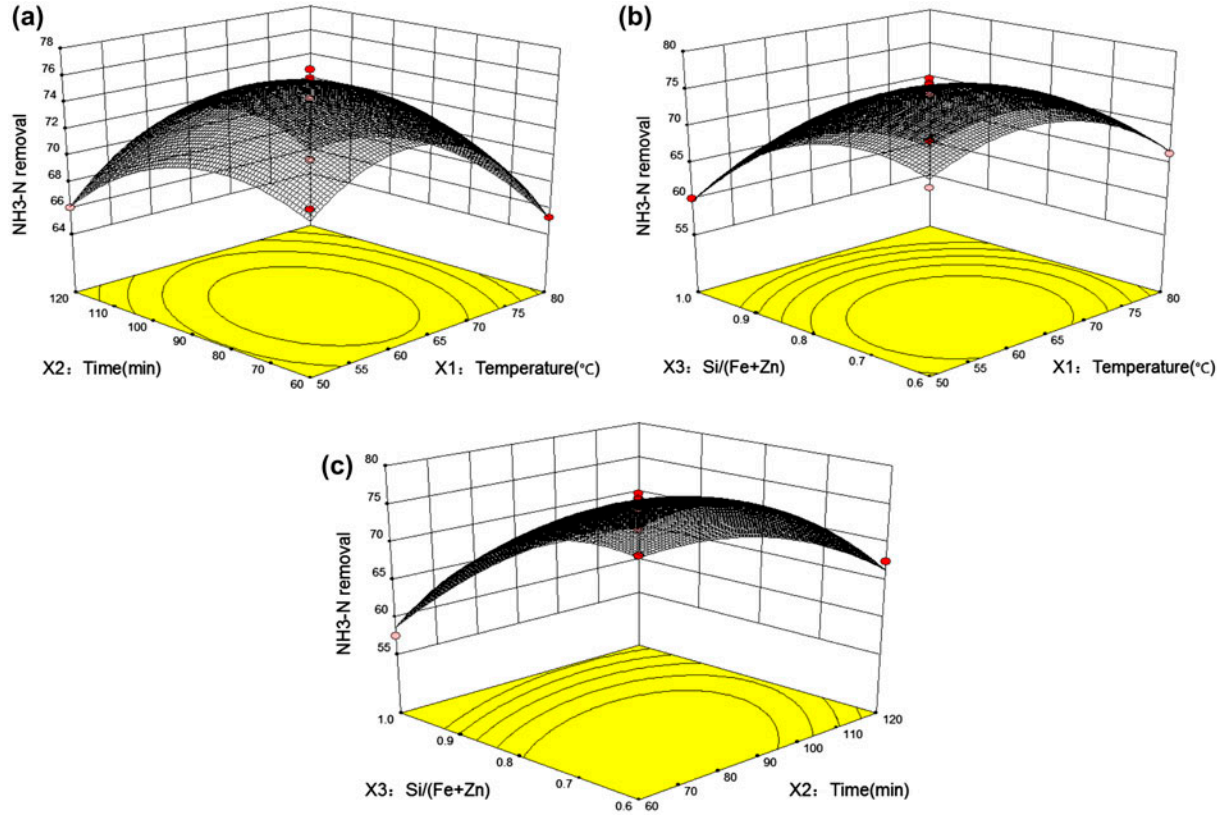

Fig. 4. Response surface for NH_3-N removal as a function of (a) temperature and time (Si/(Fe + Zn): 0.8), (b) temperature and Si/(Fe + Zn) (time: 90 min), and (c) time and Si/(Fe + Zn) (temperature: 65°C).

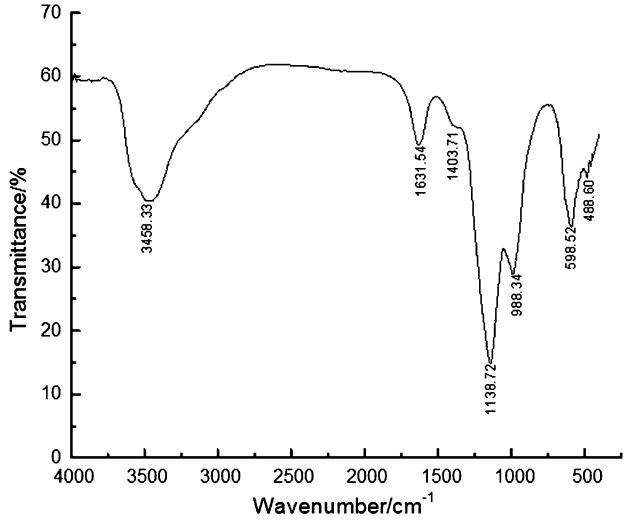

Fig. 5. IR spectra of PSFZ.

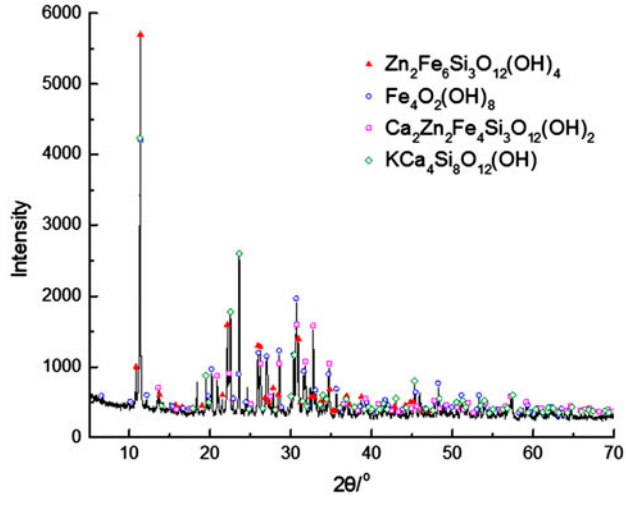

Fig. 6. XRD spectra of PSFZ.

crystalline character of PSFZ. We can see that PSFZ mainly consist of $Zn_2Fe_6Si_3O_{12}(OH)_4$, $Fe_4O_2(OH)_8$, $Ca_2Zn_2Fe_4Si_3O_{12}(OH)_2$, and $Ca_4Si_8O_{12}(OH)$, but the diffractive crystals such as ZnO, $ZnSO_4$, $Zn(OH)_2$, Fe_2O_3, Fe_3O_4, $Fe_2(SO_4)_3$, and SiO_2 are not observed. This result implies that PSFZ is complex compounds of Zn,

Fe, Si, and other ions, rather than a simple mixture of the raw materials. This explanation agrees with the suggestions by Moussas and Zouboulis [19]. In addition, some new compounds were formed (at $2\theta = 18.4^{\circ}$, 20.9°, 24.7°, 29.6°, 32.4°, 35.8°, and 45.9°), indicating that PSFZ contains new complex compounds without standard molecular formula or new matters excluded in the XRD card. In short, the XRD spectra analysis shows that PSFZ is a complex hydroxyl polymer, and agree with the conclusion of IR analysis.

3.3.3. Surface morphology

Fig. 7 displays the surface morphology of powder sample PSFZ. As shown in Fig. 7, PSFZ almost appeared to be a kind of uniform network structure consisting of some shale-like structure with small size, and the top ends of the shale-like unite were arranged densely or loosely on the structure with some gaps among them. The distances of the gaps were different from each other and some gaps were not clear. A series of pleated ditches with different width and depth were distributed among the loose structures, in which lots of protuberant parts increased the surface energy and absorption area, which would be conducive to continuous absorption of pollutants. Besides, the branch-like structure made up of small irregular units also could be detected. It implies a cross-copolymerization between Zn, Fe, and Si in PSFZ, and the branch-like units would adsorb and connect with colloidal particles in wastewater, which accelerates their sedimentation.

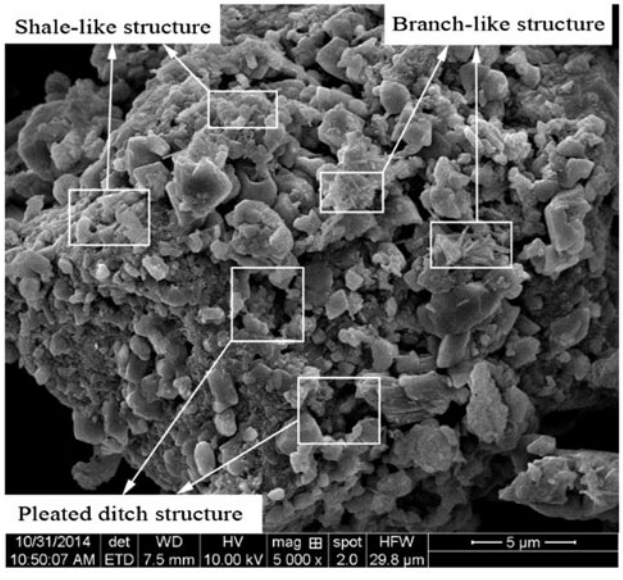

Fig. 7. Surface morphology of PSFZ.

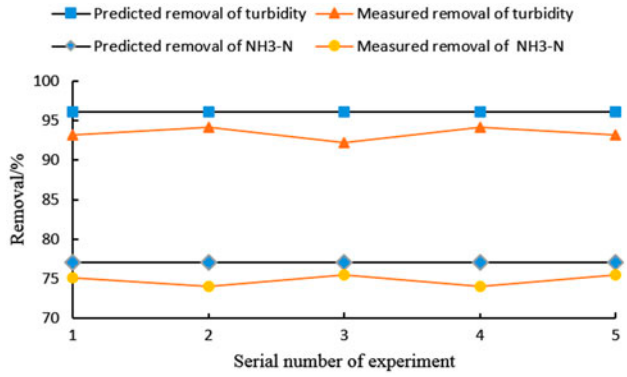

Fig. 8. Comparison between predicted and measured values.

3.4. Optimization of preparation conditions

Optimization was performed on the basis of response equations to determine the optimal synthesis conditions for PSFZ prepared. The optimal preparation conditions for maximum turbidity and NH_3-N removal efficiency (96 and 77.03%, respectively) were temperature of 65°C, time of 80 min, and Si/(Fe + Zn) moral ratio of 0.73. In addition, to confirm the validity of the regression equations, mean value interpolation was employed, by which five experiments approximated the predicted preparation conditions were obtained. For each run, three repeatability experiments were conducted and the results would be compared with those predicated by regression equations.

As shown in Fig. 8, both measured turbidity and NH_3-N removal were close to those predicted values using RSM. The relative errors of predicted and estimated values were between 2 and 4%. This testifies that RSM approach was appropriate for optimizing the preparation conditions of PSFZ coagulant.

4. Conclusions

The objective of this study was to explore the optimal preparation conditions of PSFZ coagulant on turbidity and NH_3-N removal efficiency using RSM. RSM was appropriate for determining the optimum conditions, understanding the relationships among the independent factors and response variables, and maximizing the process efficiency. The results reveal that the optimal preparation conditions were temperature of 65°C, time of 80 min, and Si/(Fe + Zn) moral ratio of 0.73, corresponding to turbidity and NH_3-N

removal percentages of 96 and 77.03, respectively. Five verification experimental runs which were obtained from regression equations using mean value interpolation were carried out, and the relative errors of the measured and predicted values were between 2 and 4%. The regression equations could be used as theoretical basis for preparation process of PSFZ on turbidity and NH_3-N removal efficiency. They are helpful to flexibly select the appropriate process parameters in the engineering applications. Furthermore, the IR and XRD spectra analysis results indicate that PSFZ is a complex compound of Zn, Fe, and Si, and morphological analysis shows that PSFZ has some shale-like, branch-like, and pleated ditch structures, which suggest that PSFZ has strong adsorption bridging ability.

Acknowledgments

This work was funded by the National Scientific Foundation China (NSFC51178207), Shandong Provincial National Science Foundation (ZR2011EEM003), and the Natural Science Foundation of Shandong Province (ZR2012EEL21, ZR2013EEL002).

References

[1] N.C. Boelee, H. Temmink, M. Janssen, C.J.N. Buisman, R.H.Wijffels, Nitrogen and phosphorus removal from municipal wastewater effluent using microalgal biofilms, Water Res. 45 (2011) 5925–5933.
[2] F.Y. Sun, X.M. Wang, X.Y. Li, An innovative membrane bioreactor (MBR) system for simultaneous nitrogen and phosphorus removal, Process Biochem. 48 (2013) 1749–1756.
[3] L.B. Chu, J.L. W, comparison of polyurethane foam and biodegradable polymer as carriers in moving bed biofilm reactor for treating wastewater with a low C/N ratio, Chemosphere 83 (2011) 63–68.
[4] S.M. Hocaoglu, G. Insel, E.U. Cokgor, D. Orhon, Effect of sludge age on simultaneous nitrification and denitrification in membrane bioreactor, Bioresour. Technol. 102 (2011) 6665–6672.
[5] G.M. Ayoub, A. Hamzeh, L. Semerjian, Post treatment of tannery wastewater using lime/bittern coagulation and activated carbon adsorption, Desalination 273 (2011) 359–365.
[6] M. Izquierdo, X. Querol, Leaching behaviour of elements from coal combustion fly ash: An overview, Int. J. Coal Geol. 94 (2012) 54–66.
[7] M. Fan, R.C. Brown, T.D. Wheelock, A.T. Cooper, M. Nomura, Y. Zhuang, Production of a complex coagulant from fly ash, Chem. Eng. J. 106 (2005) 269–277.
[8] G. Cornelis, C.A. Johnson, T.V. Gerven, C. Vandecasteele, Leaching mechanisms of oxyanionic metalloid and species in alkaline solid wastes: A review, Appl. Geochem. 23 (2008) 955–976.
[9] Y. Fu, J.C. Zhang, Y.Z. Wang, Y.Z. Yu, Resource preparation of poly-Al-Zn-Fe (PAZF) coagulant from galvanized aluminum slag: Characteristics, simultaneous removal efficiency and mechanism of nitrogen and organic matters, Chem. Eng. J. 203 (2012) 301–308.
[10] H.A. Hasan, S.R.S. Abdullah, S.K. Kamarudin, N.T. Kofli, Response surface methodology for optimization of simultaneous COD, NH_4^+-N and Mn^{2+} removal from drinking water by biological aerated filter, Desalination 275 (2011) 50–61.
[11] Y.F. Wang, K.F. Chen, L.H. Mo, J. Li, J. Xu, Optimization of coagulation-flocculation process for papermaking-reconstituted tobacco slice wastewater treatment using response surface methodology, J. Ind. Eng. Chem. 20 (2014) 391–396.
[12] R.H. Myers, D.C. Montgomery, C.M. Anderson-Cook, Response surface methodology: Process and product optimization using designed experiments, Wiley, Hoboken, NJ, 2009.
[13] M.B. Baskan, A. Pala, A statistical experiment design approach for arsenic removal by coagulation process using aluminum sulfate, Desalination 254 (2010) 42–48.
[14] M. Kasiri, H. Aleboyeh, A. Aleboyeh, Modeling and optimization of heterogeneous photo-fenton process with response surface methodology and artificial neural networks, Environ. Sci. Technol. 42 (2008) 7970–7975.
[15] X.B. Zhu, J.P. Tian, R. Liu, L.J. Chen, Optimization of fenton and electro-fenton oxidation of biologically treated coking wastewater using response surface methodology, Sep. Purif. Technol. 81 (2011) 444–450.
[16] G.C. Zhu, H.L. Zheng, W.Y. Chen, W. Fan, P. Zhang, T. Tshukudu, Preparation of a composite coagulant: Polymeric aluminum ferric sulfate (PAFS) for wastewater treatment, Desalination 285 (2012) 315–323.
[17] N.D. Tzoupanos, A.I. Zouboulis, Nobel inorganic-organic composite coagulants based on aluminium, Desalin. Water Treat. 13 (2010) 340–347.
[18] Y. Fu, S.L. Yu, Y.Z. Yu, L.P. Qiu, B. Hui, Reaction mode between Si and Fe and evaluation of optimal species in poly-silicic-ferric coagulant, J. Environ. Sci. 19 (2007) 678–688.
[19] P.A. Moussas, A.I. Zouboulis, A study on properties and coagulation behavior of modified inorganic polymeric coagulant-polyferric silicate sulphate (PFSiS), Sep. Purif. Technol. 63 (2008) 475–483.